

Serial PIB and MRI in normal, mild cognitive impairment and Alzheimer's disease: implications for sequence of pathological events in Alzheimer's disease

Clifford R. Jack, Jr,¹ Val J. Lowe,¹ Stephen D. Weigand,² Heather J. Wiste,² Matthew L. Senjem,¹ David S. Knopman,³ Maria M. Shiung,¹ Jeffrey L. Gunter,¹ Bradley F. Boeve,³ Bradley J. Kemp,¹ Michael Weiner,⁴ Ronald C. Petersen³ and the Alzheimer's Disease Neuroimaging Initiative^{1†}

1 Department of Diagnostic Radiology, Mayo Clinic and Foundation, Rochester, MN, USA

2 Division of Biomedical Statistics and Informatics, Mayo Clinic and Foundation, Rochester, MN, USA

3 Department of Neurology, Mayo Clinic and Foundation, Rochester, MN, USA

4 Department of Veterans Affairs Medical Center, University of California at San Francisco and Center for Imaging of Neurodegenerative Diseases, San Francisco, CA, USA

[†]Some of the data used in the preparation of this article were obtained from the Alzheimer's disease Neuroimaging Initiative (ADNI) database (<http://www.loni.ucla.edu/ADNI>). As such, the investigators within the ADNI contributed to the design and implementation of ADNI and/or provided data but did not participate in analysis or writing of this report. ADNI investigators include (complete listing available at www.loni.ucla.edu/ADNI/Collaboration/ADNI_Manuscript_Citations.pdf).

Correspondence to: Clifford R. Jack, Jr, MD,
Mayo Clinic,
Diagnostic Radiology,
200 First Street SW,
Rochester, MN 55905, USA
E-mail: jack.clifford@mayo.edu

The purpose of this study was to use serial imaging to gain insight into the sequence of pathologic events in Alzheimer's disease, and the clinical features associated with this sequence. We measured change in amyloid deposition over time using serial ¹¹C Pittsburgh compound B (PIB) positron emission tomography and progression of neurodegeneration using serial structural magnetic resonance imaging. We studied 21 healthy cognitively normal subjects, 32 with amnesic mild cognitive impairment and 8 with Alzheimer's disease. Subjects were drawn from two sources—ongoing longitudinal registries at Mayo Clinic, and the Alzheimer's disease Neuroimaging Initiative (ADNI). All subjects underwent clinical assessments, MRI and PIB studies at two time points, approximately one year apart. PIB retention was quantified in global cortical to cerebellar ratio units and brain atrophy in units of cm³ by measuring ventricular expansion. The annual change in global PIB retention did not differ by clinical group ($P=0.90$), and although small (median 0.042 ratio units/year overall) was greater than zero among all subjects ($P<0.001$). Ventricular expansion rates differed by clinical group ($P<0.001$) and increased in the following order: cognitively normal (1.3 cm³/year) < amnesic mild cognitive impairment (2.5 cm³/year) < Alzheimer's disease (7.7 cm³/year). Among all subjects there was no correlation between PIB change and concurrent change on CDR-SB ($r=-0.01$, $P=0.97$) but some evidence of a weak correlation with MMSE ($r=-0.22$, $P=0.09$). In contrast, greater rates of ventricular expansion were clearly correlated

with worsening concurrent change on CDR-SB ($r=0.42$, $P<0.01$) and MMSE ($r=-0.52$, $P<0.01$). Our data are consistent with a model of typical late onset Alzheimer's disease that has two main features: (i) dissociation between the rate of amyloid deposition and the rate of neurodegeneration late in life, with amyloid deposition proceeding at a constant slow rate while neurodegeneration accelerates and (ii) clinical symptoms are coupled to neurodegeneration not amyloid deposition. Significant plaque deposition occurs prior to clinical decline. The presence of brain amyloidosis alone is not sufficient to produce cognitive decline, rather, the neurodegenerative component of Alzheimer's disease pathology is the direct substrate of cognitive impairment and the rate of cognitive decline is driven by the rate of neurodegeneration. Neurodegeneration (atrophy on MRI) both precedes and parallels cognitive decline. This model implies a complimentary role for MRI and PIB imaging in Alzheimer's disease, with each reflecting one of the major pathologies, amyloid dysmetabolism and neurodegeneration.

Keywords: Alzheimer's disease; amyloid imaging; magnetic resonance imaging, longitudinal imaging; mild cognitive impairment; Pittsburgh compound B

Abbreviations: AD=Alzheimer's disease; MCI=mild cognitive impairment; CN=cognitively normal; MRI=magnetic resonance imaging; PIB= ^{11}C Pittsburgh compound B

Introduction

Alzheimer's disease pathology can be broadly thought of in three classes: (i) amyloid dysmetabolism, characterized pathologically by amyloid plaque formation (ii) neurofibrillary tangle formation, and (iii) neurodegeneration, characterized pathologically by neurofibrillary tangle formation, and ultrastructurally by loss of neurons, synapses and dendritic arborization (Braak and Braak, 1991; Terry *et al.*, 1991). Given that these qualitatively different pathologies characterize Alzheimer's disease, it is reasonable to ask if they arise simultaneously and progress in lockstep, or if they have different time courses.

Imaging modalities can be thought of as *in vivo* indicators of specific pathologies. Amyloid labelling PET ligands, such as ^{11}C Pittsburgh compound B (PIB) primarily measure brain amyloid plaque load (Klunk *et al.*, 2004; Rowe *et al.*, 2007; Drzezga *et al.*, 2008; Ikonovic *et al.*, 2008; Leinonen *et al.*, 2008) but also localize in cerebral vascular amyloid (Bacskai *et al.*, 2007; Johnson *et al.*, 2007; Lockhart *et al.*, 2007). Structural MRI, on the other hand, is an *in vivo* indicator of neurodegeneration (Bobinski *et al.*, 2000; Gosche *et al.*, 2002; Jack *et al.*, 2002; Silbert *et al.*, 2003; Csernansky *et al.*, 2004; Zarow *et al.*, 2005; Jagust *et al.*, 2008; Vemuri *et al.*, 2008; Whitwell *et al.*, 2008). Serial multi-modality imaging studies which are sensitive to the different aspects of Alzheimer's disease pathology are an ideal way to answer questions about the temporal sequencing of different pathologic features of the disease.

In this study we measured change in amyloid deposition over time using PIB PET and progression of neurodegeneration using structural MRI, with time-locked serial imaging studies. We did this in subjects who were located at three clinically definable points along the disease trajectory in Alzheimer's disease: healthy cognitively normal controls (CN), subjects with amnesic MCI (aMCI) and subjects with Alzheimer's disease. Subjects were drawn from two sources: ongoing longitudinal registries at Mayo Clinic and the Alzheimer's disease Neuroimaging Initiative (ADNI). The purpose of this study was to use serial PIB and magnetic resonance imaging to gain insight into the sequence of pathologic events in Alzheimer's disease, and the clinical features associated with this sequence.

Methods

Sources of subjects and diagnostic evaluation at Mayo

Twenty-three subjects were studied at Mayo; 10 cognitively normal, nine amnesic mild cognitive impairment and four Alzheimer's disease. Of these, all 10 cognitively normal subjects and eight of the MCI subjects were recruited from the Mayo Clinic Study of Aging (MCSA), an epidemiologic study of normal ageing and MCI in individuals aged 70–90 years in Rochester, Olmsted County, Minnesota. The remaining amnesic MCI subject and the four Alzheimer's disease subjects were drawn from the Mayo Alzheimer's disease research center (ADRC). ADRC recruitment is drawn from individuals seeking medical care at the Mayo Clinic and, therefore, these subjects were typical of those seen at a tertiary referral centre. Both the MCSA and ADRC are longitudinal studies which include serial clinical and cognitive assessments, MRI, with the recent addition of PIB studies.

At baseline, all subjects met diagnostic criteria for cognitively normal, amnesic MCI, or Alzheimer's disease. Categorization into diagnostic groups was made on a clinical basis at consensus conferences including neurologists, neuropsychologists, a neuropsychiatrist and study coordinators. Cognitively normal subjects were asymptomatic cognitively normal volunteers. Criteria for the categorization of cognitively normal were: (i) no active neurological or psychiatric disorders; (ii) some subjects may have had ongoing medical problems, yet the illnesses or their treatments did not interfere with cognitive function; (iii) normal neurological exam and (iv) were independently functioning community dwellers. Criteria for the diagnosis of amnesic MCI were those of Petersen *et al.* (2001): (i) memory complaint documented by the patient and collateral source; (ii) relatively normal general cognition; (iii) normal activities of daily living; (iv) not demented (DSM-IV) and (v) memory impaired for age and education. In general, the amnesic MCI determination is made when the memory measures fall 1.0–1.5 SD below the means for age and education appropriate individuals in our community; however, rigid cutoffs on psychometric scores were not used to establish the diagnosis of amnesic MCI which was made on clinical grounds. The diagnosis of dementia was made using DSM-IV criteria (1994), and the diagnosis of Alzheimer's disease was made using established criteria (McKhann *et al.*, 1984).

Source of subjects and diagnostic evaluation in ADNI

Thirty-eight subjects were drawn from ADNI; 11 cognitively normal, 23 amnesic MCI and four Alzheimer's disease. ADNI is a longitudinal multisite observational study of elderly cognitively normal, amnesic MCI and Alzheimer's disease subjects. Subjects are recruited using a variety of methods, including the local ADRC, memory clinics, newspaper ads, radio and other public media campaigns. MRI and clinical/psychometric assessments are performed annually in all subjects. Additional information can be found at www.ADNI-info.org. Subjects included in this study were enrolled at 11 sites that are participating in a PIB substudy.

Clinical categorization criteria for ADNI subjects were largely the same as described above for Mayo subjects. Criteria for cognitively normal subjects were: Mini Mental State Exam (MMSE) scores between 24 and 30, no memory complaints, objective memory performance in the normal range, and a clinical dementia rating (CDR) scale score of 0 (Folstein *et al.*, 1975; Morris, 1993). ADNI amnesic MCI subjects have MMSE scores in the 24–30 range, a memory complaint verified by an informant, abnormal memory function and a CDR score of 0.5 with preservation of general cognition and functional activities of daily living. Alzheimer's disease patients met published criteria for probable Alzheimer's disease (McKhann *et al.*, 1984) with MMSE scores of 20–26 and CDR scores of 0.5–1.0.

Subject inclusion and continuous measures of cognitive performance

With six exceptions, all cognitively normal, amnesic MCI and Alzheimer's disease subjects in whom serial MRI and PIB data were available from Mayo and ADNI were included in this analysis. No other criteria were used to select subjects for this study. We excluded one ADNI cognitively normal subject with periventricular infarctions in whom the serial ventricular measurements were unreliable. We excluded five ADNI subjects in whom longitudinal PIB measurements seemed unreliable. Published estimates indicate an expected test/retest reliability of $\pm 7\%$ for PIB imaging (Lopresti *et al.*, 2005; Engler *et al.*, 2006). We operated from the premise that while increases in PIB retention over time are plausible, large decreases are not. Therefore, we excluded any case where the annual decline in PIB retention exceeded 7% on the assumption that declines in PIB retention greater than 7% exceeded currently accepted limits of reproducibility and likely represented instances of unacceptable measurement error. The five cases with declines greater than 7% that were excluded were from two ADNI sites (three at one site and two at another).

For both Mayo and ADNI subjects, the Clinical Dementia Rating scale—sum of boxes (CDR-SB) was used to assess functional performance. For ADNI subjects, the MMSE was used to assess global cognitive performance. For Mayo subjects, a 38-point test, the Short Test of Mental Status (STMS) (Kokmen *et al.*, 1991), was used to assess global cognitive performance. In order to maintain consistency with ADNI data, we converted Mayo STMS scores to MMSE scores using an algorithm developed at our centre (Tang-Wai *et al.*, 2003). STMS values transformed to MMSE scores are reported simply as MMSE throughout the manuscript.

PET acquisition

For both Mayo and ADNI subjects, production of PIB and radio labelling with ^{11}C was performed as outlined by Mathis *et al.* (2003).

For Mayo subjects, at 25 min post injection, a helical CT image was obtained for attenuation correction. The PET acquisition consisted of 5 min dynamic frames from 40 to 60 min post injection. PET sinograms were iteratively reconstructed into a 256 mm FOV. The pixel size was 1.0 mm and the slice thickness 3.3 mm. Individual frames of the PIB dynamic series were realigned if motion was detected and then a mean image was created, referred to from here on as the late uptake image.

ADNI PIB studies were performed at 11 different sites. The ADNI PIB images undergo several quality control and standardization steps which are described at www.ADNI-info.org. The ADNI late uptake PIB images used in our study were the 'maximally pre-processed files' available for download. There was one significant difference between the Mayo and the ADNI PIB late uptake images; although both data sets consisted of four 5 min dynamic frames, ADNI PIB images were acquired 50–70 min post injection while the Mayo images were acquired 40–60 min post injection.

PIB image processing and atlas-based brain parcellation for quantitative PIB region of interest analysis

All PIB quantitative image analyses was performed at Mayo, using the same fully automated image processing pipeline which is described in detail (Jack *et al.*, 2008b; Senjem *et al.*, 2008). The method includes region of interest sharpening of PIB images using each subject's MRI. The automated anatomic labelling (AAL) atlas (Tzourio-Mazoyer *et al.*, 2002) was modified in-house to contain the following labelled regions of interest: right and left parietal, temporal, prefrontal, primary sensory-motor, orbito frontal, anterior cingulate, posterior cingulate/precuneus and occipital. Statistics on image voxel values were extracted from each automatically labelled cortical region of interest in the atlas. Right- and left-sided homologous PIB regions of interest demonstrate high within subject intra-class correlation; therefore, the right and left sides were combined for quantitative analyses (Jack *et al.*, 2008b; Raji *et al.*, 2008). A global cortical PIB retention summary was formed by combining the prefrontal, orbito-frontal, parietal, temporal, anterior cingulate and posterior cingulate/precuneus ratio values for each subject, using a weighted average of these regions of interest values where larger regions of interest were given greater weight. PIB ratio images were calculated by dividing the median value in each target cortical region of interest by the median value in the cerebellar grey matter region of interest of the atlas. PIB data in the manuscript are reported in cortical to cerebellar retention ratio units. Measurement of PIB retention was performed independently on the baseline and follow-up image volumes for each subject.

Throughout the results section, subjects are classified as either PIB positive or PIB negative, using a global cortical to cerebellar ratio cut point of 1.5 to separate the two groups (Jack *et al.*, 2008b). While inspection of the results will reveal that the PIB retention distribution is continuous, many leading research groups have also described their results dichotomously (positive versus negative) in order to map continuous measures of PIB retention onto typically used clinical notions of a normal versus abnormal test result (Pike *et al.*, 2007; Rabinovici *et al.*, 2007; Aizenstein *et al.*, 2008; Gomperts *et al.*, 2008; Mormino *et al.*, 2008).

MRI acquisition

MRI acquisition protocols were very similar for Mayo and ADNI subjects. There was one notable difference; although all subjects were

scanned on the same scanner at baseline and follow up, Mayo subjects were scanned at 3T while ADNI subjects were scanned at 1.5T. Mayo subjects were imaged with a 3D magnetization prepared rapid acquisition gradient echo (MPRAGE) imaging sequence developed at Mayo for the Alzheimer's Disease Neuroimaging Initiative study (Jack *et al.*, 2008a). Parameters were: sagittal plane, TR/TE/T1, 2300/3/900 ms; flip angle 8°, 26 cm field of view (FOV); 256 × 256 in-plane matrix with a phase FOV of 0.94 and slice thickness of 1.2 mm.

ADNI collects 1.5T MRI scans in all subjects and 3T scans in only 25% of the sample; therefore ADNI 1.5T MRI scans were used for this study. ADNI is a multi-site study and there are minor variations in the MRI protocol based on the specific hardware/software configuration on each scanner. The nominal parameters of the ADNI MPRAGE were: sagittal plane, TR/TE/T1, 2400/3/1000 ms, flip angle 8°, 24 cm FOV, 192 × 192 in-plane matrix, 1.2 mm slice thickness (Jack *et al.*, 2008a).

All images were corrected for image distortion due to gradient non-linearity using 'GradWarp' (Jovicich *et al.*, 2006) and for intensity inhomogeneity using 'N3' (Sled *et al.*, 1998) using a software pipeline running at Mayo. Post processing image corrections for Mayo and ADNI scans were identical since the ADNI MRI core is centred at Mayo.

MRI analysis

MRI-processing steps were performed by a research technician (MMS) who was blinded to all clinical information. Brain atrophy was assessed by measuring ventricular expansion rates using the boundary shift integral (BSI) technique (Freeborough and Fox, 1997; Gunter *et al.*, 2003). Differences were calculated in pair-wise fashion between the baseline scan and the follow up scan. Following spatial registration of the follow up scan to the baseline scan, intensity differences between the two scans at the brain-CSF boundary were used to compute change in volume. The ventricular atrophy rate was derived by creating a binary ventricular mask for each subject that selectively extracted ventricular change from the boundary shift integral. Quality control testing in our laboratory shows that the intra-class correlation coefficient for test–retest reproducibility of ventricle rate measurements from short interval serial MRI scans with this method is 0.91 which is better than whole brain boundary shift integral (Jack *et al.*, 2004). In the context of this analysis, an additional advantage of casting atrophy

as ventricular expansion rather than brain shrinkage is that biological worsening for both MRI and PIB go in the same direction (i.e. increasing values mean worse pathology). Baseline ventricular volume was measured from the ventricular mask, and was normalized for inter-subject variation in head size by dividing ventricular volume by that subject's total intra-cranial volume (TIV) as described in Jack *et al.* (1989).

Statistical methods

We used non-parametric methods to analyse numeric distributions in order to have a consistent approach to analysing these data which included skewed distributions. When comparing three groups simultaneously on numeric variables, we used the Kruskal–Wallis test. When comparing two groups, we used the Wilcoxon rank-sum test. We used Spearman rank-order correlations, which we denote simply by *r*, to evaluate associations between paired numeric measures. We analysed categorical variables using chi-squared tests with continuity correction unless one or more expected cell counts was less than one, in which case Fisher's exact test was used. We summarized numeric distributions graphically by showing individual values superimposed over a box indicating the sample median and quartiles (i.e. the 25th, 50th and 75th percentiles). All *P*-values are two-sided. We did not adjust our *P*-values for multiple comparisons (O'Brien, 1983; Perneger, 1998). A complete discussion of our rationale can be found in Perneger (1998).

Results

Demographic features by clinical group and source

When reporting results we will refer to clinical diagnostic category (cognitively normal versus amnestic MCI versus Alzheimer's disease) as clinical 'group' and will denote subjects from Mayo and ADNI as coming from different 'sources'. Clinical and demographic data are reported in Table 1, with accompanying *P* values for group and source differences in Supplementary Table E1. Age,

Table 1 Subject demographics

Characteristics	Cognitively normal		Amnestic mild cognitive impairment		Alzheimer's disease	
	ADNI	Mayo	ADNI	Mayo	ADNI	Mayo
Number of subjects	11	10	23	9	4	4
Age at first PIB exam, median (range), years	72 (63–87)	75 (72–90)	75 (61–88)	79 (72–87)	70 (68–77)	66 (54–80)
Gender, no. (%) male	8 (73)	7 (70)	14 (61)	5 (56)	3 (75)	1 (25)
Education, median (range), years	14 (12–20)	16 (12–20)	16 (12–20)	12 (12–19)	16 (12–20)	16 (13–20)
APOE, no. (%) e4 carrier ^a	2 (18)	3 (30)	14 (61)	2 (33)	1 (25)	1 (100)
MMSE, median (range)	29 (24–30)	28 (25–30)	27 (24–30)	27 (24–28)	24 (20–24)	22 (17–26)
CDR–SB, median (range) ^a	0 (0–1)	0 (0–0.5)	1.5 (0.5–4)	1.5 (0–3)	5 (4–6)	4 (1.5–6)
Months between PIB exams, median (range)	12 (11–13)	14 (14–17)	12 (9–14)	14 (12–23)	12 (9–12)	12 (9–25)
Months between MRI exams, median (range)	12 (11–13)	15 (13–17)	13 (11–15)	15 (14–23)	12 (11–12)	12 (12–28)
Diagnosis at second PIB exam, no. (%) ^a						
Cognitively normal	10 (100)	9 (90)	1 (5)	1 (11)	0	0
MCI	0	1 (10)	14 (70)	5 (56)	0	0
Alzheimer's disease	0	0	5 (25)	3 (33)	4 (100)	4 (100)

^a Missing data: three Mayo amnestic MCI and three Mayo AD subjects missing APOE e4 status; one ADNI CN missing CDR–SB; one ADNI CN and three ADNI amnestic MCI subjects missing diagnosis at second PIB exam.

education, gender, APOE e4, cognitive and functional performance distributions did not differ at the $P < 0.05$ level by source of subjects. Overall—i.e. Mayo and ADNI subjects combined—cognitively normal and amnesic MCI subjects were slightly older than Alzheimer’s disease; and APOE 4 carriers were less common in cognitively normal than in amnesic MCI subjects. Twenty-eight percent of amnesic MCI subjects progressed to a diagnosis of Alzheimer’s disease and two amnesic MCI subjects reverted to a diagnosis of cognitively normal at the time of the second imaging study. On average cognitively normal subjects performed best on the MMSE and CDR-SB, Alzheimer’s disease worst and amnesic MCI intermediate (each $P < 0.01$). Intervals between baseline and follow-up PIB and MRI studies did not differ by clinical diagnosis group; with one exception, the MRI interval was slightly greater in amnesic MCI than Alzheimer’s disease. Both PIB and MRI inter-scan intervals differed by source of subjects ($P < 0.001$) and were on average 3 months greater for Mayo compared to ADNI cognitively normal and amnesic MCI subjects.

Baseline PIB and MRI findings by clinical group and source of subjects

Baseline PIB data are illustrated in Fig. 1 and Table 2, with accompanying P values for group differences in Table 3 and for source differences in Supplementary Table E2. There were no within group differences in baseline global PIB retention between Mayo and ADNI sources (Supplementary Table E2). Among all subjects, median PIB retention values at baseline differed significantly by clinical group (overall test, $P = 0.01$) and were ordered, Alzheimer’s disease > amnesic MCI > cognitively normal (Fig. 1). Taking a global PIB cortical to cerebellar ratio value of 1.5 as a cutoff denoting PIB ‘positivity’, 6/21 (29%) cognitively normal subjects were PIB positive. Out of 32, 19 (59%) amnesic MCI subjects were PIB positive. A single ADNI subject labelled clinically as Alzheimer’s disease was PIB negative (presumably a clinical misdiagnosis). Baseline PIB retention ratio values were greater among amnesic MCI APOE 4 carriers than non-carriers ($P = 0.003$), but did not differ between carriers and non-carriers among cognitively normal and Alzheimer’s disease subjects.

Baseline MRI data are illustrated in Fig. 1 and Table 2, with accompanying P -values for group differences in Table 3, and for source differences in Supplementary Table E2. Baseline ventricular volume is expressed as a percentage of total intra-cranial

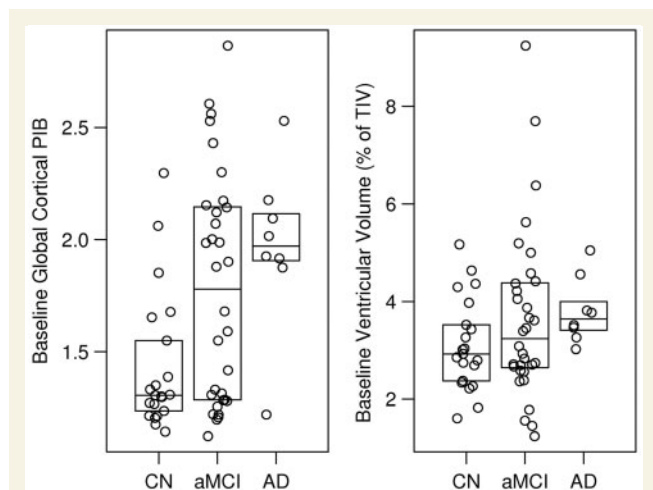


Figure 1 Baseline global cortical PIB ratio and baseline ventricular volume by clinical diagnosis. Global PIB represents a weighted average of the pre-frontal, temporal, parietal, cingulate precuneus, anterior cingulate and orbito frontal regions normalized to cerebellar retention. Baseline ventricular volume is expressed as a percentage of TIV in each subject. Boxes represent the 25th, 50th and 75th percentiles of the data. Individual points have been randomly shifted along the horizontal axis to reduce overlap.

Table 3 P -values for group-wise differences in global cortical PIB and ventricular volume

Variable	Differences among three groups ^b	Pairwise by diagnosis ^a		
		CN versus aMCI	CN versus AD	aMCI versus AD
Global cortical to cerebellar PIB ratio				
Baseline	0.01	0.02	0.003	0.40
Annual change	0.90	0.79	0.90	0.65
Ventricular volume				
Baseline volume, % of TIV	0.19	0.39	0.04	0.31
Annual change, cm ³	<0.001	0.01	<0.001	0.004

Mayo and ADNI data have been combined.
 CN = cognitively normal; aMCI = amnesic mild cognitive impairment; AD = Alzheimer’s disease.
 a Two-group Wilcoxon rank sum test.
 b Three-group Kruskal–Wallis test.

Table 2 Median (first quartile, third quartile) global cortical PIB and ventricular volume values by clinical group

Variable	Cognitively normal	Amnesic mild cognitive impairment	Alzheimer’s disease
Global cortical to cerebellar PIB ratio			
Baseline	1.3 (1.2, 1.6)	1.8 (1.3, 2.1)	2.0 (1.9, 2.1)
Annual change	0.05 (0.0, 0.10)	0.03 (−0.03, 0.12)	0.06 (0.0, 0.10)
Ventricular volume			
Baseline volume, % of TIV	2.9 (2.4, 3.5)	3.2 (2.6, 4.4)	3.6 (3.4, 4.0)
Annual change, cm ³	1.3 (0.4, 1.8)	2.5 (1.3, 4.6)	7.7 (4.0, 12.0)

Mayo and ADNI data have been combined.

volume to correct ventricular volume for inter-subject variation in head size. On average, ventricle/total intra-cranial volume values were ordered, cognitively normal > amnesic MCI > Alzheimer's disease; however, only Alzheimer's disease versus cognitively normal reached group-wise significance ($P=0.04$). Baseline ventricle/total intra-cranial volume values did not differ by source of subjects.

Rates of change in PIB retention by clinical group, source of subjects and baseline PIB retention level

Annual rate of change in global PIB retention ratio is reported in Table 2 and Fig. 2, with accompanying P values for group differences in Table 3 and for source differences in Supplementary Table E2. The annual change in global PIB retention ratio did not differ by source of subjects, $P=0.81$ (Supplementary Table E2 and illustrated in Supplementary Fig. E2). Annual rate of change in global PIB retention ratio over all groups was small (average 0.042 units/year) and did not differ by clinical group (overall, $P=0.90$) (Fig. 2, Tables 2 and 3). Annual rate of change in global PIB retention ratio was significantly greater than zero over all subjects ($P<0.001$), and individually among cognitively normal ($P=0.002$), and amnesic MCI subjects ($P=0.008$), with a trend in Alzheimer's disease ($P=0.11$). Annual rate of change in global PIB retention ratio was greater among amnesic MCI subjects who were PIB positive at baseline than those who were PIB negative ($P=0.003$); however, there was no relationship between annual rate of change in PIB retention and baseline PIB status (positive versus negative) among cognitively normal subjects.

Across all subjects the correlation between the first and second PIB measurements was very high, with an intra-class correlation

of 0.98. The intra-class correlation for ventricular volume was estimated at 0.99 suggesting that serial measures with both modalities are reliable.

Throughout this manuscript PIB retention is reported as a global cortical to cerebellar ratio which is quantified as the sum of uptake in lobar cortical regions of interest divided by a cerebellar region of interest. However, a question of interest is whether the annual change in PIB retention differs by region. To address this question, we plotted annual rate of change in PIB retention by region of interest (Supplementary Fig. E2) for 10 different cortical regions of interest with Mayo and ADNI subjects combined. There was no obvious evidence that annual rates of change in PIB retention differ by region of interest.

Rates of ventricular expansion by clinical group, source of subjects and baseline PIB retention level

Annual rate of ventricular change data are reported in Table 2 and Fig. 2, with accompanying P values for group differences in Table 3 and for source differences in Supplementary Table E2. Annual rate of ventricular change did not differ by source of subjects, overall test $P=0.24$ (Supplementary Table E2 and illustrated in Supplementary Fig. E3). Rates of ventricular enlargement differed by clinical group (overall test, $P<0.001$) and increased in the following order, cognitively normal ($1.3 \text{ cm}^3/\text{year}$) < amnesic MCI ($2.5 \text{ cm}^3/\text{year}$) < Alzheimer's disease ($7.7 \text{ cm}^3/\text{year}$). Pair-wise ventricular rate comparisons were as follows: amnesic MCI > cognitively normal ($P=0.01$); Alzheimer's disease > cognitively normal ($P<0.001$); and Alzheimer's disease > amnesic MCI ($P=0.004$). Ventricular expansion rate was greater among amnesic MCI subjects who were PIB positive at baseline than those who were PIB negative ($P=0.02$); however, there was no relationship between annual ventricular rate and baseline PIB status (positive versus negative) among cognitively normal subjects.

PIB and ventricular annual rate of change are illustrated side by side in Fig. 2 illustrating no group-wise differences in PIB rate of change but clear group-wise scaling in ventricular expansion rates. Supplementary Fig. E4 illustrates individual trajectories of PIB retention ratio and ventricular volume over time in all subjects by group. Over all subjects, the correlation between PIB rate of change and ventricular rate of change was $r=0.22$ ($P=0.10$).

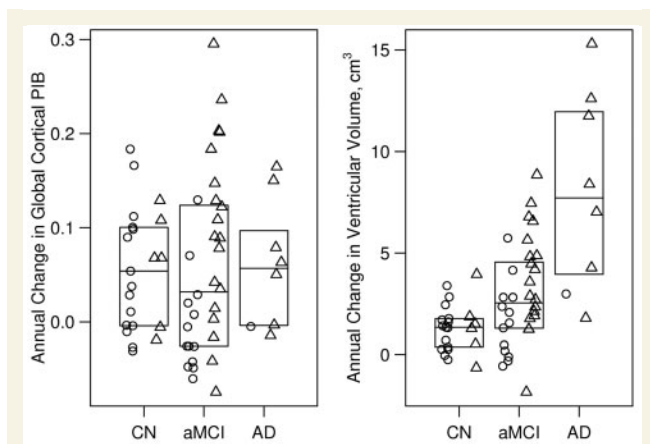


Figure 2 Annual change in global PIB ratio and ventricular volume by clinical diagnosis. Mayo and ADNI subjects have been combined. Boxes represent the 25th, 50th and 75th percentiles of the data. Individual points have been randomly shifted along the horizontal axis to reduce overlap. PIB positive subjects (baseline global cortical PIB ≥ 1.5) are represented with triangles and PIB negative subjects (baseline global cortical PIB < 1.5) are represented with circles.

Correlations between rates of change on imaging and change on continuous measures of cognitive performance

When all subjects were combined there was no correlation between PIB change and concurrent change on CDR-SB ($r=-0.01$, $P=0.97$) but perhaps some evidence of a correlation between PIB change and MMSE ($r=-0.22$, $P=0.09$). In contrast, greater rates of ventricular expansion were clearly correlated with

worsening concurrent change on CDR-SB ($r=0.42$, $P<0.01$) and MMSE ($r=-0.52$, $P<0.01$).

Discussion

The major findings from this study are as follows: (i) the PIB rate of change was small but significantly greater than zero in all subject groups; (ii) the PIB rate of change did not differ by clinical group. In contrast, ventricular rate did differ significantly by group and the group rates were ordered from greatest to least: Alzheimer's disease > mild cognitive impairment > cognitively normal; (iii) both PIB and ventricular rates of change were greater among amnesic MCI subjects who were PIB positive at baseline than amnesic MCI subjects who were PIB negative at baseline and (iv) ventricular rates of change correlated in the expected direction with concurrent change on continuous measures of cognitive and functional performance while evidence of a similar correlation with PIB rates of change was unclear.

Study characteristics

Combining Mayo and ADNI data may raise questions about the compatibility of data from these different sources. However, major demographic variables—age, education, gender, APOE e4 and cognitive and functional performance distributions—did not differ significantly between ADNI and Mayo subjects. From the imaging perspective there were differences between subjects studied at Mayo versus ADNI, the most obvious being the single versus multi site nature of the two studies. Although the MRI sequence, MPRAGE, was the same for ADNI and Mayo subjects, Mayo subjects were scanned at 3T whereas ADNI subjects were scanned at 1.5T. The acquisition window for PIB imaging was slightly different for Mayo versus ADNI subjects (40–60 versus 50–70 min post injection). However, the PIB cortical to cerebellar retention ratio plateaus between roughly 45–90 min (Lopresti *et al.*, 2005). Lopresti *et al.* (2005) found no appreciable effect of acquisition window on the difference in PIB retention levels between Alzheimer's disease patients and controls over 40–90 min.

Despite these technical imaging differences, the underlying associations between imaging and biology did not vary substantially by source of subjects. There were a number of similarities between the ADNI and the Mayo studies that likely contribute to the compatibility of data. For both ADNI and Mayo data, methods of MRI pre-processing to correct image artifacts, the boundary shift integral algorithm to calculate ventricular expansion, and PIB quantitative analyses were all performed in an identical manner using the same automated image processing pipelines at Mayo. In addition, the operational definition of amnesic MCI was the same for Mayo and ADNI subjects. This was not accidental as methods used to categorize amnesic MCI that were developed at Mayo were adopted by ADNI, and a Mayo investigator (RCP) is the leader of the ADNI clinical core. Perhaps most importantly, the compatibility of longitudinal imaging data from different sources is greatly aided by the fact that all methods were held constant within subject. Therefore, inter-subject differences in

methods tend to 'wash out' in longitudinal analyses of rates of change.

Ventricular and baseline PIB findings

Group-wise PIB retention at baseline was ordered: Alzheimer's disease > amnesic MCI > cognitively normal. Twenty-nine percent of cognitively normal and 59% of amnesic MCI subjects were PIB positive at baseline. Overall, these findings are in agreement with previously published cross-sectional PIB studies (Nordberg, 2004; Mintun *et al.*, 2006; Kemppainen *et al.*, 2007; Aizenstein *et al.*, 2008; Forsberg *et al.*, 2008; Li *et al.*, 2008; Mormino *et al.*, 2008; Sojkova *et al.*, 2008; Villemagne *et al.*, 2008).

Of greater interest are the relationships between baseline PIB and longitudinal ventricular change. Ventricular rate of change was greater in amnesic MCI subjects who were PIB positive versus PIB negative at baseline. A reasonable explanation for this combination of findings is simply that PIB positive amnesic MCI subjects do have Alzheimer's disease whereas PIB negative amnesic MCI subjects do not (Archer *et al.*, 2006; Forsberg *et al.*, 2008). This notion is reinforced by the fact that baseline PIB ratio values were significantly greater among amnesic MCI APOE 4 carriers than non-carriers. PIB negative amnesic MCI subjects by definition do have a (mild) cognitive impairment and therefore must have one or more specific pathologies underlying the impairment; however, the pathologies must be something other than Alzheimer's disease. Logical candidates include cerebrovascular disease, hippocampal sclerosis or Lewy body disease (Bennett *et al.*, 2005; Jicha *et al.*, 2006; Schneider *et al.*, 2007). None of these non-Alzheimer's disease pathologies are strongly associated with rapid rates of brain atrophy, whereas Alzheimer's disease is (Whitwell *et al.*, 2007). Therefore, the data on baseline PIB and longitudinal ventricular change in amnesic MCI are concordant overall in the following sense. Alzheimer's disease-like features clustered together—PIB positivity at baseline, high prevalence of APOE 4 carriers and rapid rates of brain atrophy. Likewise, non-Alzheimer's disease like features clustered together—PIB negativity at baseline, low prevalence of APOE 4 carriers, and slower rates of brain atrophy.

We note that although baseline ventricular/total intra-cranial volume ratio values were ordered in the expected manner, cognitively normal > amnesic MCI > Alzheimer's disease, only Alzheimer's disease versus cognitively normal reached pair-wise significance ($P=0.04$). In our experience, the ventricle boundary shift integral is an excellent MRI measure of change over time and, therefore, this was our choice of MRI metrics for longitudinal assessment (Jack *et al.*, 2004). However, cross-sectional ventricular measures are not particularly good indicators of disease severity at a fixed point in time (Jack *et al.*, 2005). The focus of this article is longitudinal measures of change. Baseline ventricular/total intra-cranial volume values were included in the manuscript only to create data presentation symmetry with baseline PIB values which were of interest (specifically their relationship with longitudinal PIB and MRI change). Had the article required a cross-sectional MRI measure at baseline with the strongest association with disease severity, we would have used the hippocampus, not the ventricle (Jack *et al.*, 1992).

Longitudinal imaging findings

The major objective of this study was to evaluate concurrent MRI, PIB and clinical change in the same subjects. Annual change in MRI was expressed in units of volume (cm^3) and annual change in PIB retention was expressed as cortical to cerebellar ratio units. While these two metrics are unfortunately not directly comparable, these are the natural units of measurement for each of the two modalities. Rates of ventricular expansion differed significantly by group and were ordered: Alzheimer's disease > amnesic MCI > cognitively normal, which implies acceleration in atrophy rate as Alzheimer's disease progresses clinically. We recognize that detecting rate acceleration at the individual subject level requires three or more separate measurements and we have two measurements per subject in this study. However, earlier studies, in which three or more unique measurements per subject were performed, demonstrated acceleration in brain atrophy rates with clinical progression of the disease (Chan *et al.*, 2003; Ridha *et al.*, 2006; Carlson *et al.*, 2008; Jack *et al.*, 2008c). When cognition was expressed as a continuous variable, concurrent measures of cognitive change mapped well onto ventricular rate of change. These longitudinal MRI findings are in agreement with an accepted body of literature indicating good correlation between rate of change in brain volume and concurrent clinical course (Fox *et al.*, 2000; Jack *et al.*, 2000). In contrast, there was no apparent correlation between PIB rate of change and CDR-SB, and minimal evidence of a correlation between PIB rate of change and MMSE. The two serial PIB studies published to date have both been in Alzheimer's disease subjects, and reported no appreciable change in PIB retention over 2 years (Engler *et al.*, 2006; Edison *et al.*, 2007). CSF AB 1–42 is inversely correlated with PIB retention (Fagan *et al.*, 2006), and therefore literature on CSF AB 1–42 is relevant to a discussion of the relationships between brain amyloid load and clinical disease expression. Inferences about the relationship between CSF AB 1–42 and longitudinal disease progression have been mixed (Clark *et al.*, 2003; Wahlund and Blennow, 2003; Hampel *et al.*, 2004; de Leon *et al.*, 2006; Hansson *et al.*, 2006; Engelborghs *et al.*, 2007; Fagan *et al.*, 2007; Sluimer *et al.*, 2008). However, Andreasen *et al.* (1999) found no relationship between CSF AB 1–42 and clinical disease duration (a proxy for disease severity) in Alzheimer's disease subjects. Mirroring this finding, Ingelsson *et al.* (2004) found no relationship between quantitative measures of cortical amyloid deposition at autopsy and duration of clinical disease in Alzheimer's disease subjects. The net conclusion that can be drawn from this literature is that an individual's amyloid load accumulates prior to clinical symptoms and reaches a plateau with no further accumulation as the disease progresses clinically—i.e. amyloid load does not increase in parallel with clinical disease progression. Our findings agree with this model of disease to an extent, however, while we found average rates of change in PIB were quite small, they were positive and not zero.

We found that PIB rate of change did not differ significantly by clinical group, which suggests a linear rate of PIB accumulation over time, at least late in life which was the age range of the subjects we studied. It is possible that the rate of PIB (amyloid deposition) is linear throughout life. At the rate we measured,

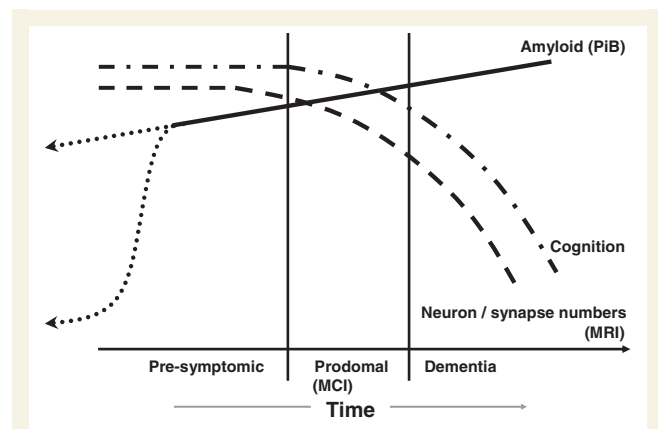


Figure 3 Proposed model relating imaging, pathology and clinical presentation over an individual's adult lifetime. The lifetime clinical course of the disease is divided into pre-symptomatic, prodromal and dementia phases. Neurodegeneration, detected by MRI, is indicated by a dashed line. Cognitive function is indicated by a dot-dash line. Amyloid deposition, detected by PIB, is indicated by a solid line late in life (i.e. that portion of the disease for which we have data). The time course of amyloid deposition early in life is represented as two possible theoretical trajectories (dotted lines), reflecting uncertainty about the time course of early PIB deposition.

0.042 ratio units per year, it would take 23.8 years to move from a negative PIB scan (cortical to cerebellar retention ratio units = 1.0) to the average level measured in Alzheimer's disease subjects (2.0 ratio units). Given our subjects' ages, generally 60s through 80s, this would mean that if amyloid accumulation proceeded linearly, amyloid deposition in patients with typical late-onset Alzheimer's disease would have to begin in subjects in their 40s. In contrast to this model, others (Ingelsson *et al.*, 2004) have proposed that the rate of amyloid deposition changes over the course of the disease, specifically, that amyloid deposition rate is rapid early and later flattens to a plateau, after a threshold is reached. Although our data do not seem to fit this non-linear model, we recognize that we do not have data that address rates of PIB (amyloid) accumulation in middle age and earlier. Figure 3 illustrates a model relating change on PIB, MRI and clinical performance over time. The dotted lines in the early portion of the amyloid curve indicate two possible trajectories which reflect our uncertainty about this period in the disease course. However, our data are consistent with a model in which amyloid deposition proceeds at a slow linear rate late in life.

Imaging as an indicator of the time dependent pathological changes in Alzheimer's disease

Our data are consistent with a model of typical late-onset Alzheimer's disease that has two main features, illustrated in Fig. 3: (i) dissociation between the rate of amyloid deposition and the rate of neurodegeneration late in life, with amyloid

deposition proceeding at a constant slow rate while neurodegeneration accelerates; and (ii) clinical symptoms are coupled to neurodegeneration not amyloid deposition. While significant plaque deposition occurs prior to clinical changes (Mintun *et al.*, 2006; Aizenstein *et al.*, 2008), neurodegeneration (indicated by atrophy on MRI) both precedes and parallels cognitive decline. The presence of brain amyloidosis alone is not sufficient to produce cognitive impairment, as evidenced by data in the current study as well as other independent studies that have consistently found significant PIB retention in up to 1/3 of cognitively normal elderly subjects (Mintun *et al.*, 2006; Aizenstein *et al.*, 2008; Gomperts *et al.*, 2008; Jack *et al.*, 2008b; Mormino *et al.*, 2008). The neurodegenerative element of Alzheimer's disease pathology is the direct substrate of cognitive impairment and the rate of cognitive decline is driven by the rate of neurodegeneration, a relationship also recently proposed by Mormino *et al.* (2008). Evidence for this is our finding that ventricular rate of change is correlated with concurrent change in cognitive and functional performance, while PIB rate of change is not. This model of disease implies a complimentary role for MRI and PIB imaging clinically, with each reflecting one of the major pathologies in Alzheimer's disease, amyloid dysmetabolism and neurodegeneration. It also implies a complimentary role in clinical trials. Longitudinal measures with MRI might be preferred as an outcome measure to detect change in the underlying neurodegenerative pathology that tracks with clinical disease stage. Conversely, PIB would be invaluable for selecting subjects for amyloid modifying therapeutic trials.

Supplementary material

Supplementary material is available at *Brain* online.

Acknowledgements

The Alexander Family Alzheimer's Disease Research Professorship of the Mayo Foundation, USA.

Funding

National Institute on Aging (P50 AG16574, U01 AG06786, R01 AG11378 and AG024904); Robert H. and Clarice Smith and Abigail Van Buren Alzheimer's Disease Research Program of the Mayo Foundation, USA.

References

- Aizenstein HJ, Nebes RD, Saxton JA, Price JC, Mathis CA, Tsopelas ND, et al. Frequent amyloid deposition without significant cognitive impairment among the elderly. *Arch Neurol* 2008; 65: 1509–17.
- American Psychiatric Association. Diagnostic and statistical manual of mental disorders, DSM-IV. Washington, DC: American Psychiatric Association; 1994.
- Andreasen N, Hesse C, Davidsson P, Minthon L, Wallin A, Winblad B, et al. Cerebrospinal fluid beta-amyloid(1-42) in Alzheimer disease: differences between early- and late-onset Alzheimer disease and stability during the course of disease. *Arch Neurol* 1999; 56: 673–80.
- Archer HA, Edison P, Brooks DJ, Barnes J, Frost C, Yeatman T, et al. Amyloid load and cerebral atrophy in Alzheimer's disease: an 11C-PIB positron emission tomography study. *Ann Neurol* 2006; 60: 145–7.
- Bacskaï BJ, Frosch MP, Freeman SH, Raymond SB, Augustinack JC, Johnson KA, et al. Molecular imaging with Pittsburgh Compound B confirmed at autopsy: a case report. *Arch Neurol* 2007; 64: 431–4.
- Bennett DA, Schneider JA, Bienias JL, Evans DA, Wilson RS. Mild cognitive impairment is related to Alzheimer disease pathology and cerebral infarctions. *Neurology* 2005; 64: 834–41.
- Bobinski M, de Leon MJ, Wegiel J, Desanti S, Convit A, Saint Louis LA, et al. The histological validation of post mortem magnetic resonance imaging-determined hippocampal volume in Alzheimer's disease. *Neuroscience* 2000; 95: 721–5.
- Braak H, Braak E. Neuropathological staging of Alzheimer-related changes. *Acta Neuropathol* 1991; 82: 239–59.
- Carlson NE, Moore MM, Dame A, Howieson D, Silbert LC, Quinn JF, et al. Trajectories of brain loss in aging and the development of cognitive impairment. *Neurology* 2008; 70: 828–33.
- Chan D, Janssen JC, Whitwell JL, Watt HC, Jenkins R, Frost C, et al. Change in rates of cerebral atrophy over time in early-onset Alzheimer's disease: longitudinal MRI study. *Lancet* 2003; 362: 1121–2.
- Clark CM, Xie S, Chittams J, Ewbank D, Peskind E, Galasko D, et al. Cerebrospinal fluid tau and beta-amyloid: how well do these biomarkers reflect autopsy-confirmed dementia diagnoses? *Arch Neurol* 2003; 60: 1696–702.
- Csernansky JG, Hamstra J, Wang L, McKeel D, Price JL, Gado M, et al. Correlations between antemortem hippocampal volume and postmortem neuropathology in AD subjects. *Alzheimer Dis Assoc Disord* 2004; 18: 190–5.
- Leon MJ, DeSanti S, Zinkowski R, Mehta PD, Pratico D, Segal S, et al. Longitudinal CSF and MRI biomarkers improve the diagnosis of mild cognitive impairment. *Neurobiol Aging* 2006; 27: 394–401.
- Drzezga A, Grimmer T, Henriksen G, Stangier I, Perneczky R, Diehl-Schmid J, et al. Imaging of amyloid plaques and cerebral glucose metabolism in semantic dementia and Alzheimer's disease. *Neuroimage* 2008; 39: 619–33.
- Edison P, Archer HA, Hinz R, Hammers A, Pavese N, Tai YF, et al. Amyloid, hypometabolism, and cognition in Alzheimer disease: an [11C]PIB and [18F]FDG PET study. *Neurology* 2007; 68: 501–8.
- Engelborghs S, Sleegers K, Cras P, Brouwers N, Serneels S, De Leenheir E, et al. No association of CSF biomarkers with APOEε4, plaque and tangle burden in definite Alzheimer's disease. *Brain* 2007; 130: 2320–6.
- Engler H, Forsberg A, Almkvist O, Blomquist G, Larsson E, Savitcheva I, et al. Two-year follow-up of amyloid deposition in patients with Alzheimer's disease. *Brain* 2006; 129: 2856–66.
- Fagan AM, Mintun MA, Mach RH, Lee SY, Dence CS, Shah AR, et al. Inverse relation between in vivo amyloid imaging load and cerebrospinal fluid Aβ42 in humans. *Ann Neurol* 2006; 59: 512–9.
- Fagan AM, Roe CM, Xiong C, Mintun MA, Morris JC, Holtzman DM. Cerebrospinal fluid tau/beta-amyloid(42) ratio as a prediction of cognitive decline in nondemented older adults. *Arch Neurol* 2007; 64: 343–9.
- Folstein MF, Folstein SE, McHugh PR. "Mini-mental state". A practical method for grading the cognitive state of patients for the clinician. *J Psychiatr Res* 1975; 12: 189–98.
- Forsberg A, Engler H, Almkvist O, Blomquist G, Hagman G, Wall A, et al. PET imaging of amyloid deposition in patients with mild cognitive impairment. *Neurobiol Aging* 2008; 29: 1456–65.
- Fox NC, Cousens S, Scahill R, Harvey RJ, Rossor MN. Using serial registered brain magnetic resonance imaging to measure disease progression in Alzheimer disease: power calculations and estimates of sample size to detect treatment effects. *Arch Neurol* 2000; 57: 339–44.

- Freeborough PA, Fox NC. The boundary shift integral: an accurate and robust measure of cerebral volume changes from registered repeat MRI. *IEEE Trans Med Imaging* 1997; 16: 623–9.
- Gomperts SN, Rentz DM, Moran E, Becker JA, Locascio JJ, Klunk WE, et al. Imaging amyloid deposition in Lewy body diseases. *Neurology* 2008; 71: 903–10.
- Gosche KM, Mortimer JA, Smith CD, Markesbery WR, Snowdon DA. Hippocampal volume as an index of Alzheimer neuropathology: findings from the Nun Study. *Neurology* 2002; 58: 1476–82.
- Gunter JL, Shiung MM, Manduca A, Jack CR, Jr. Methodological considerations for measuring rates of brain atrophy. *J Magn Reson Imaging* 2003; 18: 16–24.
- Hampel H, Mitchell A, Blennow K, Frank RA, Brettschneider S, Weller L, et al. Core biological marker candidates of Alzheimer's disease – perspectives for diagnosis, prediction of outcome and reflection of biological activity. *J Neural Transm* 2004; 111: 247–72.
- Hansson O, Zetterberg H, Buchhave P, Londos E, Blennow K, Minthon L. Association between CSF biomarkers and incipient Alzheimer's disease in patients with mild cognitive impairment: a follow-up study. *Lancet Neurol* 2006; 5: 228–34.
- Ikonomic MD, Klunk WE, Abrahamson EE, Mathis CA, Price JC, Tsopelas ND, et al. Post-mortem correlates of in vivo PiB-PET amyloid imaging in a typical case of Alzheimer's disease. *Brain* 2008; 131: 1630–45.
- Ingelsson M, Fukumoto H, Newell KL, Growdon JH, Hedley-Whyte ET, Frosch MP, et al. Early A β accumulation and progressive synaptic loss, gliosis, and tangle formation in AD brain. *Neurology* 2004; 62: 925–31.
- Jack CR, Jr, Bernstein MA, Fox NC, Thompson P, Alexander G, Harvey D, et al. The Alzheimer's Disease Neuroimaging Initiative (ADNI): MRI methods. *J Magn Reson Imaging* 2008a; 27: 685–91.
- Jack CR, Jr, Dickson DW, Parisi JE, Xu YC, Cha RH, O'Brien PC, et al. Antemortem MRI findings correlate with hippocampal neuropathology in typical aging and dementia. *Neurology* 2002; 58: 750–7.
- Jack CR, Jr, Lowe VJ, Senjem ML, Weigand SD, Kemp BJ, Shiung MM, et al. 11C PiB and structural MRI provide complementary information in imaging of Alzheimer's disease and amnesic mild cognitive impairment. *Brain* 2008b; 131: 665–80.
- Jack CR, Jr, Petersen RC, O'Brien PC, Tangalos EG. MR-based hippocampal volumetry in the diagnosis of Alzheimer's disease. *Neurology* 1992; 42: 183–8.
- Jack CR, Jr, Petersen RC, Xu Y, O'Brien PC, Smith GE, Ivnik RJ, et al. Rates of hippocampal atrophy correlate with change in clinical status in aging and AD. *Neurology* 2000; 55: 484–89.
- Jack CR, Jr, Shiung MM, Gunter JL, O'Brien PC, Weigand SD, Knopman DS, et al. Comparison of different MRI brain atrophy rate measures with clinical disease progression in AD. *Neurology* 2004; 62: 591–600.
- Jack CR, Jr, Shiung MM, Weigand SD, O'Brien PC, Gunter JL, Boeve BF, et al. Brain atrophy rates predict subsequent clinical conversion in normal elderly and amnesic MCI. *Neurology* 2005; 65: 1227–31.
- Jack CR, Jr, Twomey CK, Zinsmeister AR, Sharbrough FW, Petersen RC, Cascino GD. Anterior temporal lobes and hippocampal formations: normative volumetric measurements from MR images in young adults. *Radiology* 1989; 172: 549–54.
- Jack CR, Jr, Weigand SD, Shiung MM, Przybelski SA, O'Brien PC, Gunter JL, et al. Atrophy rates accelerate in amnesic mild cognitive impairment. *Neurology* 2008c; 70: 1740–52.
- Jagust WJ, Zheng L, Harvey DJ, Mack WJ, Vinters HV, Weiner MW, et al. Neuropathological basis of magnetic resonance images in aging and dementia. *Ann Neurol* 2008; 63: 72–80.
- Jicha GA, Parisi JE, Dickson DW, Johnson K, Cha R, Ivnik RJ, et al. Neuropathologic outcome of mild cognitive impairment following progression to clinical dementia. *Arch Neurol* 2006; 63: 674–81.
- Johnson KA, Gregas M, Becker JA, Kinnecom C, Salat DH, Moran EK, et al. Imaging of amyloid burden and distribution in cerebral amyloid angiopathy. *Ann Neurol* 2007; 62: 229–34.
- Jovicich J, Czanner S, Greve D, Haley E, van der Kouwe A, Gollub R, et al. Reliability in multi-site structural MRI studies: effects of gradient non-linearity correction on phantom and human data. *Neuroimage* 2006; 30: 436–43.
- Kemppainen NM, Aalto S, Wilson IA, Nagren K, Helin S, Bruck A, et al. PET amyloid ligand [11C]PiB uptake is increased in mild cognitive impairment. *Neurology* 2007; 68: 1603–6.
- Klunk WE, Engler H, Nordberg A, Wang Y, Blomqvist G, Holt DP, et al. Imaging brain amyloid in Alzheimer's disease with Pittsburgh Compound-B. *Ann Neurol* 2004; 55: 306–19.
- Kokmen E, Smith GE, Petersen RC, Tangalos E, Ivnik RC. The short test of mental status. Correlations with standardized psychometric testing. *Arch Neurol* 1991; 48: 725–8.
- Leinonen V, Alafuzoff I, Aalto S, Suotunen T, Savolainen S, Nagren K, et al. Assessment of beta-amyloid in a frontal cortical brain biopsy specimen and by positron emission tomography with carbon 11-labeled Pittsburgh Compound B. *Arch Neurol* 2008; 65: 1304–9.
- Li Y, Rinne JO, Mosconi L, Pirraglia E, Rusinek H, DeSanti S, et al. Regional analysis of FDG and PiB-PET images in normal aging, mild cognitive impairment, and Alzheimer's disease. *Eur J Nucl Med Mol Imaging* 2008; 35: 2169–81.
- Lockhart A, Lamb JR, Osredkar T, Sue LI, Joyce JN, Ye L, et al. PiB is a non-specific imaging marker of amyloid-beta (A β) peptide-related cerebral amyloidosis. *Brain* 2007; 130: 2607–15.
- Lopresti BJ, Klunk WE, Mathis CA, Hoge JA, Ziolkowski SK, Lu X, et al. Simplified quantification of Pittsburgh Compound B amyloid imaging PET studies: a comparative analysis. *J Nucl Med* 2005; 46: 1959–72.
- Mathis CA, Wang Y, Holt DP, Huang GF, Debnath ML, Klunk WE. Synthesis and evaluation of 11C-labeled 6-substituted 2-arylbenzothiazoles as amyloid imaging agents. *J Med Chem* 2003; 46: 2740–54.
- McKhann G, Drachman D, Folstein M, Katzman R, Price D, Stadlan EM. Clinical diagnosis of Alzheimer's disease: report of the NINCDS-ADRDA Work Group under the auspices of Department of Health and Human Services Task Force on Alzheimer's Disease. *Neurology* 1984; 34: 939–44.
- Mintun MA, Larossa GN, Sheline YI, Dence CS, Lee SY, Mach RH, et al. [11C]PiB in a nondemented population: potential antecedent marker of Alzheimer disease. *Neurology* 2006; 67: 446–52.
- Mormino EC, Kluth JT, Madison CM, Rabinovici GD, Baker SL, Miller BL, et al. Episodic memory loss is related to hippocampal-mediated {beta}-amyloid deposition in elderly subjects. *Brain* 2008; Ahead of print. ISSN 1460-2156; doi:10.1093/brain/awn320 (published online 28 November 2008).
- Morris JC. The Clinical Dementia Rating (CDR): current version and scoring rules. *Neurology* 1993; 43: 2412–4.
- Nordberg A. PET imaging of amyloid in Alzheimer's disease. *Lancet Neurol* 2004; 3: 519–27.
- O'Brien PC. The appropriateness of analysis of variance and multiple-comparison procedures. *Biometrics* 1983; 39: 787–94.
- Perneger TV. What's wrong with Bonferroni adjustments. *Bmj* 1998; 316: 1236–8.
- Petersen RC, Doody R, Kurz A, Mohs RC, Morris JC, Rabins PV, et al. Current concepts in mild cognitive impairment. *Arch Neurol* 2001; 58: 1985–92.
- Pike KE, Savage G, Villemagne VL, Ng S, Moss SA, Maruff P, et al. Beta-amyloid imaging and memory in non-demented individuals: evidence for preclinical Alzheimer's disease. *Brain* 2007; 130: 2837–44.
- Rabinovici GD, Furst AJ, O'Neil JP, Racine CA, Mormino EC, Baker SL, et al. 11C-PiB PET imaging in Alzheimer disease and frontotemporal lobar degeneration. *Neurology* 2007; 68: 1205–12.
- Raji CA, Becker JT, Tsopelas ND, Price JC, Mathis CA, Saxton JA, et al. Characterizing regional correlation, laterality and symmetry of amyloid deposition in mild cognitive impairment and Alzheimer's disease with Pittsburgh Compound B. *J Neurosci Methods* 2008; 172: 277–82.

- Ridha BH, Barnes J, Bartlett JW, Godbolt A, Pepple T, Rossor MN, et al. Tracking atrophy progression in familial Alzheimer's disease: a serial MRI study. *Lancet Neurol* 2006; 5: 828–34.
- Rowe CC, Ng S, Ackermann U, Gong SJ, Pike K, Savage G, et al. Imaging beta-amyloid burden in aging and dementia. *Neurology* 2007; 68: 1718–25.
- Schneider JA, Arvanitakis Z, Bang W, Bennett DA. Mixed brain pathologies account for most dementia cases in community-dwelling older persons. *Neurology* 2007; 69: 2197–204.
- Senjem ML, Lowe V, Kemp B, Weigand S, Knopman D, Boeve B, et al. Automated ROI analysis of 11C Pittsburgh compound B images using structural magnetic resonance imaging atlases. *Alzheimer's Dementia* 2008; 4 (Suppl 1).
- Silbert LC, Quinn JF, Moore MM, Corbridge E, Ball MJ, Murdoch G, et al. Changes in premorbid brain volume predict Alzheimer's disease pathology. *Neurology* 2003; 61: 487–92.
- Sled JG, Zijdenbos AP, Evans AC. A nonparametric method for automatic correction of intensity nonuniformity in MRI data. *IEEE Trans Med Imaging* 1998; 17: 87–97.
- Sluimer JD, Bouwman FH, Vrenken H, Blankenstein MA, Barkhof F, van der Flier WM, et al. Whole-brain atrophy rate and CSF biomarker levels in MCI and AD: A longitudinal study. *Neurobiol Aging* 2008; Ahead of print. ISSN 1558-1497.
- Sojkova J, Beason-Held L, Zhou Y, An Y, Kraut MA, Ye W, et al. Longitudinal cerebral blood flow and amyloid deposition: an emerging pattern? *J Nucl Med* 2008; 49: 1465–71.
- Tang-Wai DF, Knopman DS, Geda YE, Edland SD, Smith GE, Ivnik RJ, et al. Comparison of the short test of mental status and the mini-mental state examination in mild cognitive impairment. *Arch Neurol* 2003; 60: 1777–81.
- Terry RD, Masliah E, Salmon DP, Butters N, DeTeresa R, Hill R, et al. Physical basis of cognitive alterations in Alzheimer's disease: synapse loss is the major correlate of cognitive impairment. *Ann Neurol* 1991; 30: 572–80.
- Tzourio-Mazoyer N, Landeau B, Papathanassiou D, Crivello F, Etard O, Delcroix N, et al. Automated anatomical labeling of activations in SPM using a macroscopic anatomical parcellation of the MNI MRI single-subject brain. *Neuroimage* 2002; 15: 273–89.
- Vemuri P, Whitwell JL, Kantarci K, Josephs KA, Parisi JE, Shiung MS, et al. Antemortem MRI based STRUCTURAL Abnormality INDEX (STAND)-scores correlate with postmortem Braak neurofibrillary tangle stage. *Neuroimage* 2008; 42: 559–67.
- Villemagne VL, Pike KE, Darby D, Maruff P, Savage G, Ng S, et al. Abeta deposits in older non-demented individuals with cognitive decline are indicative of preclinical Alzheimer's disease. *Neuropsychologia* 2008; 46: 1688–97.
- Wahlund LO, Blennow K. Cerebrospinal fluid biomarkers for disease stage and intensity in cognitively impaired patients. *Neurosci Lett* 2003; 339: 99–102.
- Whitwell JL, Jack CR, Jr, Parisi JE, Knopman DS, Boeve BF, Petersen RC, et al. Rates of cerebral atrophy differ in different degenerative pathologies. *Brain* 2007; 130: 1148–58.
- Whitwell JL, Josephs KA, Murray ME, Kantarci K, Przybelski SA, Weigand SD, et al. MRI correlates of neurofibrillary tangle pathology at autopsy: a voxel-based morphometry study. *Neurology* 2008; 71: 743–9.
- Zarow C, Vinters HV, Ellis WG, Weiner MW, Mungas D, White L, et al. Correlates of hippocampal neuron number in Alzheimer's disease and ischemic vascular dementia. *Ann Neurol* 2005; 57: 896–903.